NEACRP-L-192
(USA)
June 1977

SIMULATION OF AN HCDA SEQUENCE ON THE ZPPR CRITICAL FACILITY

R.E. Kaiser, C.L. Beck and M.J. Lineberry

Argonne National Laboratory
P.O. Box 2528, Idaho Falls, Idaho 83401

ABSTRACT

ZPPR Assembly 5 was used to simulate successive stages in a loss-of-flow initiated Hypothetical Core Disruptive Accident: sodium-voiding, clad redistributions, and fuel redistribution. Each stage was subdivided into steps corresponding to the anticipated accident sequence. The reactivity change in each step was measured, and reaction rate and small-sample reactivity distributions were measured in each of the three accident stages. The measurements were adequately predicted using diffusion theory, with some transport and streaming corrections.

INTRODUCTION

The experimental program in assembly 5 of the Argonne Zero Power Plutonium Reactor (ZPPR) included simulation of stages of an LMFBR Hypothetical Core Disruptive Accident (HCDA). The data provide static benchmark parameters against which to test the calculational methods proposed for prediction of the consequences of severe disruptive accidents.

Since ZPPR-5 is part of a series of engineering mockup critical experiments for the Clinch River Breeder Reactor (CRBR), the size and composition of the assembly was close to that of CRBR. The HCDA measurements were planned by examining the significant steps of an accident sequence initiatied by a loss of coolant flow. This was done by constructing sequential, static configurations of an accident in progress. Included are the progressive voiding of sodium in several axial and radial steps, then steel slumping in a central voided zone, and finally fuel rearrangement in a section of the steel slump zone. The sequence was done for two different configurations representing beginning-of-cycle (BOC) and end-of-cycle (EOC) conditions.

HCDA EXPERIMENTS

ZPPR is a split-table machine in which large fast reactors can be simulated. Zones of different composition are constructed by arrangement of plates within drawers. The flexibility of this system was very important in the HCDA measurements.

In order to accomplish adjustments of excess reactivity in assembly 5 without modifying the hexagonal core outline, extra fuel plates were added to selected core drawers, replacing U_3O_8. By proper selection of the location and

number of such fuel spikes, reactivity adjustments ranging from a few cents to several dollars were made.

The sodium-void patterns consisted of four radial zones voided sequentially as shown in Fig. 1. Each radial zone was voided in several axial steps as shown in Fig. 2, simulating the void pattern to be expected in the hypothetical loss of flow situation. The worth of each successive change was determined from calibrated control rod positions, with minor corrections for temperature and other effects. The excess reactivity was kept within limits by modifications of the spiking pattern, with a new reference configuration established for each change in the spiking pattern.

In phase A, the third radial zone included areas around the flat portions of the hexagon, in the higher flux regions of the outer core. In phase B, the mockup rods were inserted at those positions which resulted in local flux depressions. Therefore, the void pattern in the outer core zone was modified to follow voiding in the higher flux regions. Also, the phase B measurements in zones one and two included an additional axial step near the lower core/axial blanket interface to define the axial void worths in more detail.

In preparation for the steel-slumping measurements, iron oxide plates in the zone in question were replaced by iron plates of a size appropriate to conserve the total iron mass. The oxygen content was thus lowered, but the movement of the iron plates as part of the steel slumping was then accomplished without coincident movement of oxygen. In the simulation of the clad-melting stage of the HCDA, all steel or iron that could be moved by itself (Na void cans and Fe plates in Fig. 3) was removed from the steel depleted zones. As shown in Fig. 3, an equivalent amount of steel was added in the heavy steel zone to simulate freezing of the molten metal.

The phase A measurements included an intermediate step with steel-depletion to 229 mm (9 in.) above and below the midplane, and freezing between 229 and 305 mm (9 and 12 in.). The final phase A step and the phase B measurement involved depletion to ±356 mm (14 in.) from the midplane and freezing between 356 and 457 mm (14 and 18 in.), also shown in Fig. 3. The total mass of steel moved in the 356 mm slump was 496.4 g, a 29% reduction in the steel-depleted zone. The measurement technique used was the same as for the sodium voiding, with the steel-slumping accomplished in four steps.

Two different sequences were performed in phase A to simulate fuel melting. First, all of the fuel between ±356 mm (14 in.) of the reactor midplane in the zone in Fig. 1d was slumped to ±178 mm (7 in.) of the midplane. The second measurement reversed the procedure, with no fuel in the ±178 mm region and double fuel between 178 and 356 mm on either side of the midplane. The measurements were done in two radial steps in phase A, progressing outward. Each step was the equivalent of one subassembly ring of CRBR, where four ZPPR drawers are treated as equivalent to one subassembly. In the phase B measurements, which included a mockup control rod in the central position, the outer ring of the zone was slumped first, simulating an outward shift in the peak power because of the control rod.

Again, the same measurement techniques were used as described for sodium-voiding. In both the fuel- and steel-slumping, stainless steel spacers were used in voided regions of the core to prevent materials from moving. The effect of the spacers is included in the steel mass figures for the steel-slump experiment, but no correction was made to the fuel slump data to account for the small steel movement involving spacers and fuel clad.

In each of the sodium-void, 356 mm steel-slump, and fuel slump-out configurations, small sample reactivity traverses were run in the radial and axial

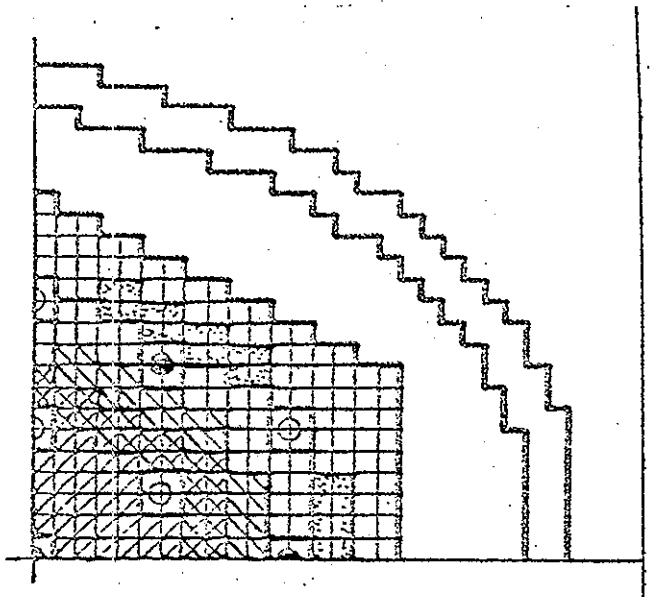

ZONE 1 ZONE 2

a) SODIUM-VOID ZONE, PHASE A

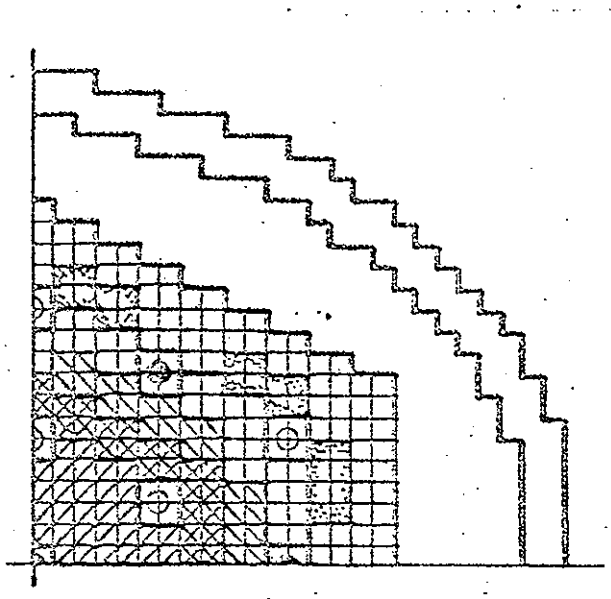

ZONE 3 ZONE 4

b) SODIUM-VOID ZONE, PHASE B

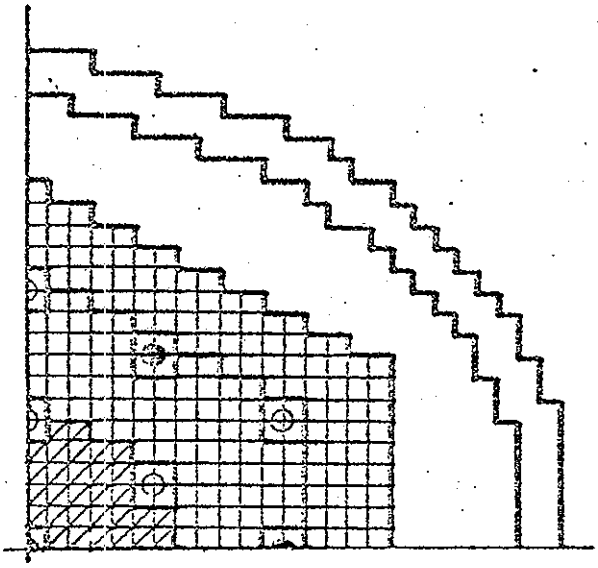

c) STEEL-SLUMP ZONE

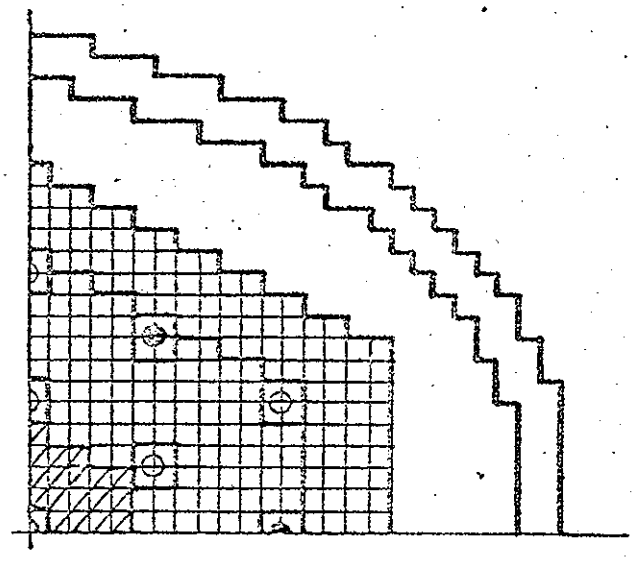

d) FUEL SLUMP ZONE

CR's PARKED IN BOTH PHASES

CR's PARKED IN 5A INSERTED IN 5B

Fig. 1 Zone Outlines for Sodium Void, Steel Slump, and Fuel Slump Experiments in the ZPPR Assembly 5 HCDA Simulation.

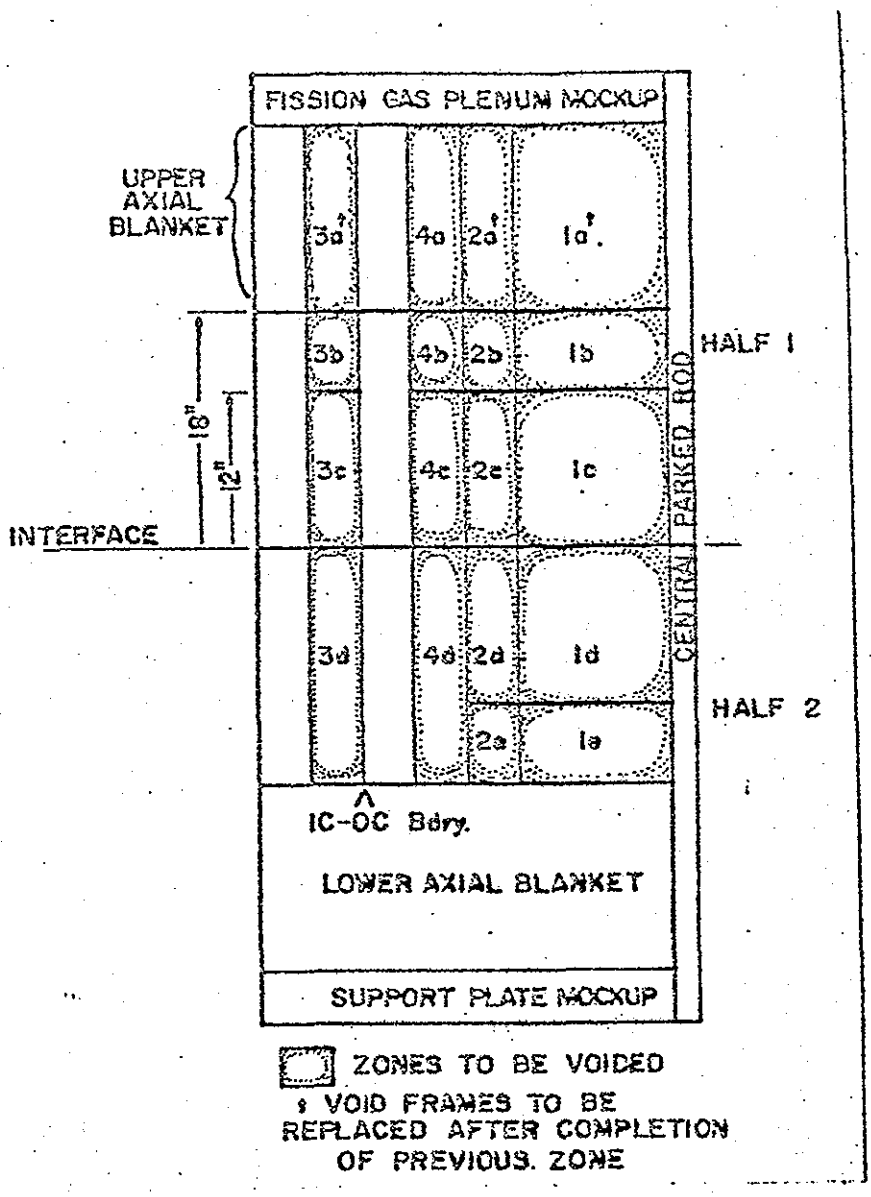

Fig. 2 Axial Zones of Sodium-Voiding Sequence in the ZPPR Assembly 5 HCDA Simulation.

directions, the axial traverses extending over the full height of the core. The samples included the ^{239}Pu, ^{238}U, ^{10}B, and stainless steel, with ^{240}Pu, ^{235}U, and ^{252}Cf included in the fuel slumped configurations. In addition, radial and axial $^{235}U(n,f)$ foil traverses were performed at the same points in the program.

A more detailed discussion of the experimental procedures is available elsewhere [1].

METHOD OF CALCULATION

The use of plate materials and metallic fuel results in a system which is more heterogeneous than the power reactor fueled with mixed oxide pins. The heterogeneity effects are important to an understanding of the measurements in ZPPR-5. These effects are accounted for in two separate but related treatments.

Heterogeneity effects for each cell type were treated with the MC^2-II and SDX codes [2,3]. Resonance self shielding was calculated using equivalence theory and flux fine structure by an integral transport-perturbation method. A 156-group, intermediate, library was collapsed to 28 groups using an infinite medium spectrum for each composition. ENDF/B Version IV cross section data were employed throughout.

The second heterogeneity effect associated with the plate construction involves streaming within the plates. Matrix tubes that are filled with drawers

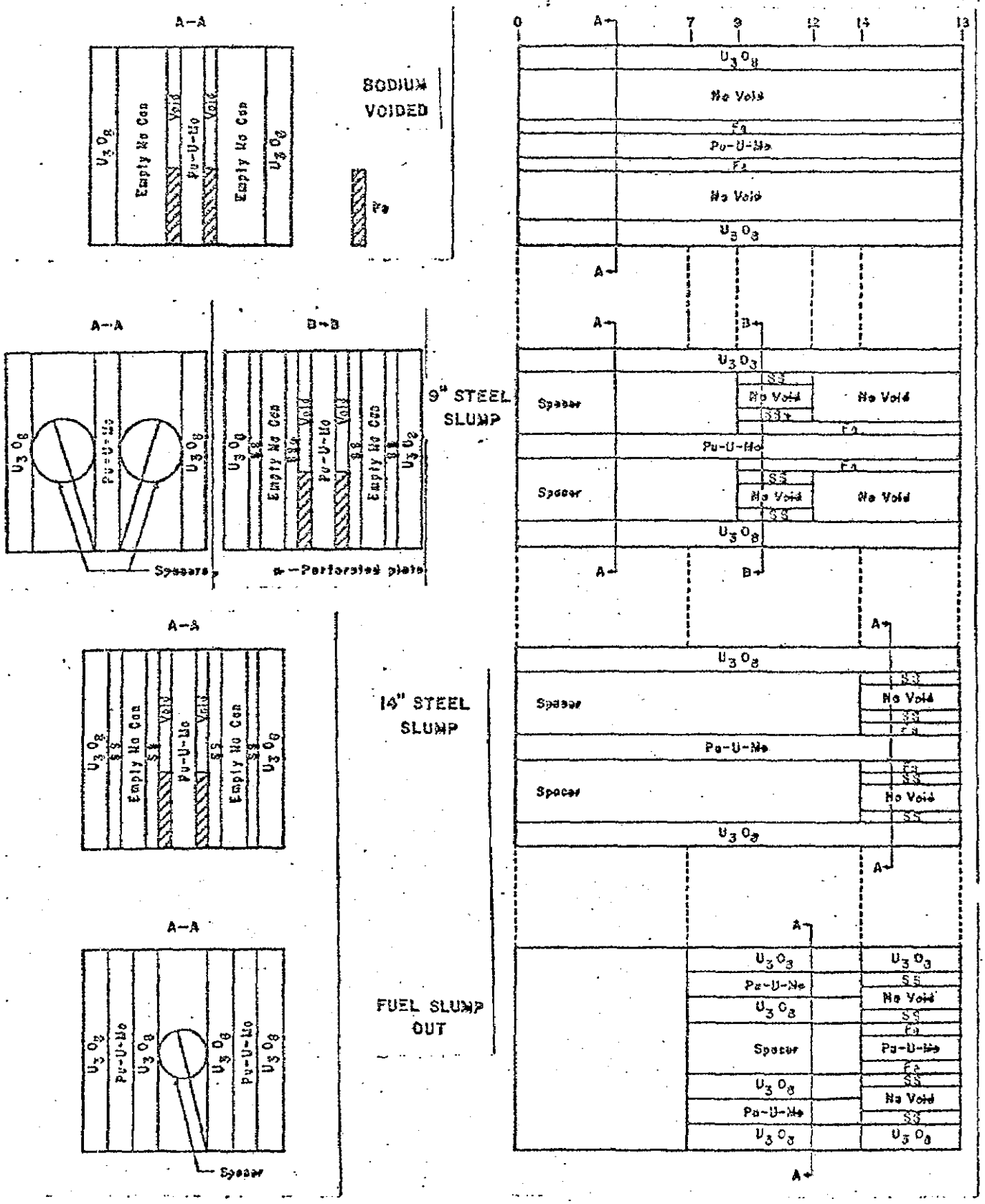

Fig. 3 Drawer Configurations Used in the Stages of the ZPPR Assembly 5 HCDA Simulation.

of identical construction create planes within the assembly. When these planes consist of relatively transparent materials such as sodium, stainless steel, or actual voids, significant streaming occurs. The Benoist procedure [4] of employing directionally-dependent diffusion coefficients has been tentatively adopted to account for this effect.

Two-dimensional (rz geometry) diffusion and perturbation calculations were used to analyze the measurements. The calculations employed modules within the Argonne Reactor Computation System [5]. All reactivity worths were calculated using exact perturbation techniques so that a component breakdown (leakage and non-leakage) of the reactivity would be available. A mesh spacing of about 50 mm was selected. Special calculations were done in several instances to assess the impact of using transport theory (S_4P_0) calculations with the DOT-III code [6] or a reduced mesh size.

EVALUATION OF SODIUM VOID REACTIVITIES

The results of the sodium void measurements and basic diffusion calculations (exact perturbation) are shown in Table I. First-order perturbation calculations were also done, and the results were generally in adequate agreement with the exact perturbation results shown. A more detailed discussion of sodium-void analysis at Argonne is included in another paper at this meeting [7].

From Table I it is apparent that rz models are not adequate for calculating void reactivities in zones where off-center control rods are present. Observe the residual in calculation (C) and experiment (E) for calculations of ZPPR-5A (no inserted rods) and the central zones of ZPPR-5B. Compare this with the C-E for the third zone of the latter assembly. These problems have been observed in previous void calculations at ZPPR. Considering only zones 1 and 2, the distribution of C-E values indicates no bias resulting from the inserted rods.

Use of directional diffusion coefficients to account for streaming uniformly decreases the calculated reactivity because of an increase of approximately 40% in the (negative) leakage term. The new C-E values are distributed about zero, but the spread is essentially the same as with no streaming correction. Because of modeling problems mentioned above, only zones 1 and 2 have been analyzed with streaming corrections.

The conclusion of the analysis of sodium void experiments in the HCDA simulation is that streaming corrections are significant. Although indications are that the Benoist procedure somewhat overestimates the effect [7], it has been adopted for present use. Since streaming is much greater in the critical assembly, measured data must be adjusted before they are used to predict void coefficients for the power reactor. Calculations then provide good estimates of the resultant sodium-void reactivity over several zones of different radial position and height.

EVALUATION OF STEEL SLUMP REACTIVITIES

Results of the measurements and diffusion calculations of the steel slump reactivities are shown in Table II. Again the calculations are of the exact perturbation type, but do not greatly differ from first-order perturbation results. Standard diffusion coefficients were used in these simple calculations, and provide a consistent C/E ratio of about 1.10, with no apparent bias due to control rods (no difference in C/E between phase A and phase B), and no apparent streaming effect (the two axial slump positions in phase A have C/E ratios which are almost the same). Thus streaming must affect the steel reference and steel slumped cases about equally. The conclusion is that simple calculations do a surprisingly good job of predicting steel slump reactivities, even though the reactivities involved exceed 1$.

TABLE I

ZPPR Assembly 5 HCDA Void-zone Calculations

Void Step[a]	Experiment, ¢	Sodium Mass, kg	Calculated, ¢	C-E	C-E[b]
Phase A					
1A[c]	-14.8 ± 0.2	46.20	-9.0	5.8	-3.9
1B	-22.9 ± 0.2	19.71	-13.4	9.6	-1.9
1C	29.6 ± 0.3	39.39	42.4	12.7	3.5
1D	25.5 ± 0.3	59.10	44.3	18.8	5.3
2A[c]	-10.3 ± 0.3	36.53	-6.0	4.3	-2.6
2B	-14.4 ± 0.3	15.58	-9.3	5.1	-3.0
2C	18.1 ± 0.3	31.15	30.6	12.5	6.7
2D	14.9 ± 0.3	46.74	31.1	16.2	7.1
3A[c]	-5.8 ± 0.2	37.11	-4.1	1.7	
3B	-11.1 ± 0.4	15.46	-7.8	3.3	
3C	-1.2 ± 0.4	30.94	6.5	7.7	
3D	-8.6 ± 0.2	46.40	2.4	11.0	
4A[c]	-9.1 ± 0.2	36.50	-5.3	3.8	
4B	-13.7 ± 0.2	15.67	-8.3	5.4	
4C	12.2 ± 0.2	31.32	24.6	12.4	
4D	8.1 ± 0.2	46.98	23.8	15.7	
Phase B					
1A	-18.3 ± 0.4	46.20	-13.4	4.9	-5.1
1B	-18.4 ± 0.3	19.71	-12.7	5.7	-6.5
1C	40.6 ± 0.4	39.39	55.4	14.8	4.8
1D[d]	52.7 ± 0.2	39.39	65.4	12.7	7.3
1E[d]	-13.5 ± 0.3	19.71	-7.5	6.0	3.7
2A	-13.9 ± 0.3	36.53	-9.6	4.3	-2.9
2B	-15.7 ± 0.2	15.58	-10.5	5.2	-3.5
2C	24.0 ± 0.3	31.15	33.4	9.4	3.5
2D[d]	31.0 ± 0.3	31.15	39.2	8.2	5.3
2E[d]	-11.6 ± 0.3	15.58	-6.9	4.7	-2.1
3A	-6.1 ± 0.3	37.11	-3.7	2.4	
3B	-8.0 ± 0.3	15.46	-2.3	5.7	
3C	-0.4 ± 0.3	30.94	23.9	24.3	
3D	-7.4 ± 0.3	46.40	18.9	26.3	
4A[c]	-4.0 ± 0.3	36.50	-1.1	2.9	
4B	-11.8 ± 0.3	15.67	-8.2	3.6	
4C	18.2 ± 0.3	31.32	27.2	9.0	
4D	10.3 ± 0.3	46.98	25.5	15.2	

[a] Refer to Fig. 2 for definition of step.

[b] C-E values calculated using Benoist diffusion coefficients.

[c] Increase in steel mass of ~20 kg in each zone will cause systematic bias in the results. Calculations consider this effect.

[d] In phase B, the bottom half of the core was voided in two steps in regions 1 and 2.

TABLE I

ZPPR Assembly 5 HCDA Void-zone Calculations

Void Step[a]	Experiment, ¢	Sodium Mass, kg	Calculated, ¢	C-E	C-E[b]
Phase A					
1A[c]	-14.8 ± 0.2	46.20	-9.0	5.8	-3.9
1B	-22.9 ± 0.2	19.71	-13.4	9.6	-1.9
1C	29.6 ± 0.3	39.39	42.4	12.7	3.5
1D	25.5 ± 0.3	59.10	44.3	18.8	5.3
2A[c]	-10.3 ± 0.3	36.53	-6.0	4.3	-2.6
2B	-14.4 ± 0.3	15.58	-9.3	5.1	-3.0
2C	18.1 ± 0.3	31.15	30.6	12.5	6.7
2D	14.9 ± 0.3	46.74	31.1	16.2	7.1
3A[c]	-5.8 ± 0.2	37.11	-4.1	1.7	
3B	-11.1 ± 0.4	15.46	-7.8	3.3	
3C	-1.2 ± 0.4	30.94	6.5	7.7	
3D	-8.6 ± 0.2	46.40	2.4	11.0	
4A[c]	-9.1 ± 0.2	36.50	-5.3	3.8	
4B	-13.7 ± 0.2	15.67	-8.3	5.4	
4C	12.2 ± 0.2	31.32	24.6	12.4	
4D	8.1 ± 0.2	46.98	23.8	15.7	
Phase B					
1A	-18.3 ± 0.4	46.20	-13.4	4.9	-5.1
1B	-18.4 ± 0.3	19.71	-12.7	5.7	-6.5
1C[d]	40.6 ± 0.4	39.39	55.4	14.8	4.8
1D[d]	52.7 ± 0.2	39.39	65.4	12.7	7.3
1E[d]	-13.5 ± 0.3	19.71	-7.5	6.0	3.7
2A	-13.9 ± 0.3	36.53	-9.6	4.3	-2.9
2B	-15.7 ± 0.2	15.58	-10.5	5.2	-3.5
2C[d]	24.0 ± 0.3	31.15	33.4	9.4	3.5
2D[d]	31.0 ± 0.3	31.15	39.2	8.2	5.3
2E[d]	-11.6 ± 0.3	15.58	-6.9	4.7	-2.1
3A	-6.1 ± 0.3	37.11	-3.7	2.4	
3B	-8.0 ± 0.3	15.46	-2.3	5.7	
3C	-0.4 ± 0.3	30.94	23.9	24.3	
3D	-7.4 ± 0.3	46.40	18.9	26.3	
4A[c]	-4.0 ± 0.3	36.50	-1.1	2.9	
4B	-11.8 ± 0.3	15.67	-8.2	3.6	
4C	18.2 ± 0.3	31.32	27.2	9.0	
4D	10.3 ± 0.3	46.98	25.5	15.2	

[a] Refer to Fig. 2 for definition of step.

[b] C-E values calculated using Benoist diffusion coefficients.

[c] Increase in steel mass of ∿20 kg in each zone will cause systematic bias in the results. Calculations consider this effect.

[d] In phase B, the bottom half of the core was voided in two steps in regions 1 and 2.

TABLE II

Summary of Steel Slumping Analysis for Assembly 5, Phases A and B

Zone Description	Experimental (E) Worth, ¢	Calculated (C) Worth, ¢	C/E
Phase A			
Steel out 0-229 mm in each half, Heavy Steel 229-305 mm, each half	38.78 ± 0.45	43.53	1.122
Steel out 0-356 mm in each half, Heavy Steel 356-457 mm, each half	106.66 ± 1.06	116.87	1.096
Phase B			
Steel out 0-356 mm in each half, Heavy Steel 356-457 mm, each half	101.43 ± 0.38	111.20	1.096

TABLE III

ZPPR-5 Fuel Slump Reactivities

ZPPR-5, Phase A		
Fuel Slump Inward		
Basic Diffusion	$1.655	
Benoist Correction	0.084	
Transport Correction	0.034	
Corrected Calculation (C)	1.773	
Estimated Uncertainty in Calculation		± 0.100
Measured Value (E)	1.799	± 0.009
C-E	-0.026	± 0.100
Fuel Slump Outward		
Basic Diffusion	$-0.562	
Benoist Correction	0.140	
Transport Correction	0.158	
Corrected Calculation (C)	-0.264	
Estimated Uncertainty in Calculation		± 0.100
Measured Value (E)	-0.086	± 0.002
C-E	-0.178	± 0.100
ZPPR-5, Phase B		
Fuel Slump Outward		
Basic Diffusion	$-0.679	
Benoist Correction	0.153	
Transport Correction	0.153	
Corrected Calculation (C)	-0.373	
Estimated Uncertainty in Calculation		± 0.120
Measured Value (E)	-0.231	± 0.003
C-E	-0.142	± 0.120

EVALUATION OF FUEL SLUMP REACTIVITIES

The reactivities associated with rearranging the heavy metal (and associated oxygen in U_3O_8) are shown in Table III. Only end-points are shown, and the reactivities of several intermediate steps are also available [1]. If first-order perturbation calculations were adequate, the slump-inward and slump-outward reactivities should be of roughly equal magnitude and opposite sign. That the magnitudes differ so much in ZPPR-5, phase A indicates first-order perturbation results will fail. Such a result might also have been anticipated from ^{252}Cf small-sample traverses which were done in the slump-outward configuration. These experiments, which measure $\int dE\chi(E)\phi^*(\vec{r},E)$ [8,9], indicate the adjoint flux shifts dramatically from the reference to the slump-outward case.

The zone from which the heavy metal is removed contains only the empty drawer and matrix tube, and this tenuous material requires a transport calculation for specification of the neutron flux. Since diffusion theory was treated as the basic method, transport calculations were considered as a correction. Moreover, an appreciable streaming correction was anticipated in this analysis, and this too was treated as a correction with separate diffusion calculations using Benoist diffusion coefficients. As shown in Table III, both effects reduce the discrepancy between the basic calculation and the measured values. What results is a C-E bias of -3¢ for the slump-inward case of ZPPR-5, phase A, and about -16¢ for the two slump-outward cases.

Estimates of uncertainties in the calculated value have been made, and the cumulative result is shown. Some sources of this uncertainty are mesh and quadrature used in an rz geometric model, use of Benoist streaming corrections, and use of infinite medium calculations in cross section preparation. The result is an uncertainty of 10-12¢, and the C-E values are consistent within these bounds.

Because the fuel slump measurements involve rearrangement of core heavy metal in the right mix for criticality, it would seem reasonable that the C/E should be unity (provided as-built assemblies have k's calculated near unity), and this is true for the fuel slump-inward case. The C-E bias for the fuel slump-outward case is consistent with past axial small-sample C/E results for ^{238}U and ^{239}Pu. It is found that the C/E ratio for ^{239}Pu worth gets smaller as the distance from the midplane increases, while for ^{238}U the C/E gets larger. Table IV shows this typical behavior from ZPPR assembly 3, phase 1B. Observe that the C/E ratios for these two materials diverge monotonically. The conclusion is that the higher C-E bias in the fuel slump-outward case is probably not due to an inherent difficulty in the HCDA simulation, but rather is present in more routine experiments.

TABLE IV

Axial Small Sample Reactivity Data ZPPR Assembly 3, Phase 1B, Corrected for Plate Streaming

Distance from Midplane, in.	Pu-30[a] C/E	DU-6[a] C/E
3.78	1.20	1.52
6.00	1.19	1.55
8.22	1.20	1.56
10.43	1.17	1.60
12.65	1.16	1.59
14.86	1.15	1.82
17.08	1.12	2.09

[a]The Pu-30 sample is 97.2 wt% ^{239}Pu, and the DU-6 sample is 99.78 wt% ^{238}U. Corrections for impurities were made in calculated values.

CONCLUSION

In the analysis of sodium-voiding, streaming effects were found to be significant in the critical assemblies, and measured data must be corrected before they can be used to predict power reactor void coefficients. In the steel slumping analysis, the streaming effects between the reference and slumped cases appeared to cancel, leading to the conclusion that simple calculations can do a good job of predicting the measured reactivities. The C-E bias in the fuel slump-out measurement is consistent with past experience with ^{239}Pu and ^{238}U axial small-sample measurements, and is probably not due to an inherent difficulty in the experiment.

The ZPPR assembly 5 experiments demonstrate that critical assemblies can be used to study the neutronics of an HCDA, and should be of considerable value in scoping HCDA measurement sequences adaptable to other core designs. The results are adequately predicted using diffusion and transport theory and standard multigroup processing techniques.

REFERENCES

1. R.E. KAISER and C.L. BECK, "Measurement and Analysis of the HCDA Simulation in ZPPR Assembly 5," ANL-76-109 (to be published).

2. H. HENRYSON II, B.J. TOPPEL and C.G. STENBERG, "MC^2-2: A code to Calculate Fast Neutron Spectra and Multi-group Cross Sections," ANL-8144, Argonne National Laboratory. (1976)

3. W.M. STACEY, JR., et al, "A New Space Dependent Fast-Neutron Multigroup Cross Section Preparation Capability," *Trans. Am. Nucl. Soc.*, 15, p. 292 (1972).

4. P. BENOIST, "Streaming Effects and Collision Probabilities in Lattices," *Nucl. Sci. Eng.*, 34, p. 285 (1968).

5. B.J. TOPPEL, Ed., "The Argonne Reactor Computation (ARC) System," ANL-7332, Argonne National Laboratory (Nov. 1972).

6. W.A. RHOADES and F.R. MYNATT, "The DOT-III Two-Dimensional Discrete Ordinates Transport Code," ORNL-TM-4280, Oak Ridge National Laboratory (Sept. 1973).

7. C.L. BECK et al, "On the Extrapolation of ZPR Sodium Void Measurements to the Power Reactor," these proceedings.

8. S.G. CARPENTER and R.W. GOIN, "Measured Kinetic Parameters for ZPPR Assembly 2," Applied Physics Division Annual Report, ANL-8010, p. 181, Argonne National Laboratory (1972).

9. R.A. KARAM, "Measurements of the Normalization Integral and the Spatial Distribution of the Importance of Fission Neutrons," *Nucl. Sci. Eng.*, 37, p. 192 (1969).